NUMERICAL ANALYSIS OF THE 3-D TURBULENT FLOW IN AN S-SHAPED DIFFUSER

Q. Lin
Xiamen University, Xiamen, China
R.W.Guo
Nanjing Aeronautical Institute, Nanjing, China

Abstract

This paper presents a numerical analysis for three-dimensional turbulent flow in an S-shaped diffuser. The coordinate transformation was made because of the section variation along the duct, in order to overcome the fundamental difficulty of the computational mesh with the boundary conditions. The conservative Navier-Stokes equations is still in conservation after transformation from (x,θ,z) to (ξ,ζ,η) coordinates. And the three-dimensional body-fitted meshes have been generated. As an instance, the three-dimensional turbulent flow field in a rectangular-round S-shaped inlet has been analysed numerically. The finite-difference method, improved SIMPLE procedure and two equation $k-\varepsilon$ turbulence model are adopted for computing the flow situation. The computational results obtained agree fairly satisfactorily with experimental data, including static pressure distribution along the walls, main flow velocity profile at different section of the duct and total pressure coefficients and cross flow velocity vectors at outlet.

I. Introduction

The subsonic diffuser is a feature of inlet installations for jet aircrarft. In the case of the inlet located in the belly and offset possitions of military aircraft in the fuselage of which the engine is carried, the subsonic diffuser is tailored the S-shaped duct to conform with constraints imposed by other aspects of the aircraft design. In addition, the cross-section of the inlets often varies along the duct from arbitrary shape, for example rectangle, to circle facing the engine. In the ducts, the flow pattern is very complicated and should be paid close attention to. A considerable difficulty in calculation of the flow is the compatibility of the computational mesh with the boundary conditions. Obviously, the flow situation in the ducts of this sort puts a significant task to the computational fluid dynamics.

In previous work of the numerical investigations, references (1) and (2) dealt with potential flows in the ducts with arbitrary section. Some viscous flows in the duct with regular cross-section for example rectangle, circle or ellipse, were also analyzed[3]~[6]. The flow pattern in complicated duct computed by the method of combining potential and stream functions is given in reference(7). And a viscous analysis with parabolized Navier-Stokes equations for flows through various inlets has been made in Lewis Research Center[8].

It is not easy to analyse above flow problem in orthogonal coordinates. A numerical procedure is advanced here to predict the flow in S-shaped duct with varible cross-sections. As an instance, the three-dimensional turbulent flow field in a rectangular-round S-shaped inlet (See Fig.1) has been computed numerically. A coordinate transformation is made in order to remove the puzzler of the computational mesh compatible with the boundary conditions in the calculation at arbitrarily shaped region. A series of transformation relations is presented by tensor analysis. The governing equations of the flow are still in conservation after the transformation. Based on the coordinate transformation, the three-dimensional body-fitted meshes have been generated through the numerical solution of elliptic partial differential equations. The finite-difference method and improved SIM-

PLE procedure are used in the numerical approach. The two equation k–ε turbulence model is employed for describing the turbulent property of the duct flow. The singularity point at the centre of each section of the duct has been treated numerically during generating the body–fitted mesh and calculating the flow field. The computational results obtained agree fairly satisfactorily with experimental data, including static pressure distribution along the walls, main flow velocity profile at different sections of the duct, total pressure coefficients and cross flow velocity vectors at outlet. The study shows that the methods of coordinate transformation and grid generation are successful, and the mathematical model and the numerical method are practicable for the three–dimensional turbulent flow in the duct with arbitrary sections.

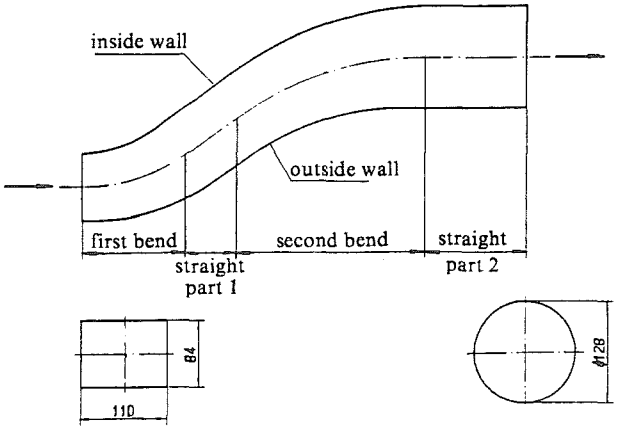

Fig.1 Sketch of the S–duct model

II. Coordinate Transformation

The orthogonal cylindrical coordinates (x,θ, z) (See Fig.2) are suitable for the internal flow through a plane S–duct with rectangular section[5]. Obviously, the problem occurs when the cross–sections of the duct are not rectangular because the boundary grids of the duct do not coincide with the numerical mesh of the flow field in cylindrical coordinates. It brings trouble in treating boundary conditions in computing. On the other hand, the accuracy of the calculation as well as numerical stability and convergency would be reduced too. To get rid of the difficulty, the coordinate transformation and grid generation in accordance with the section variation and S–shape of the duct are necessary for the numerical computation.

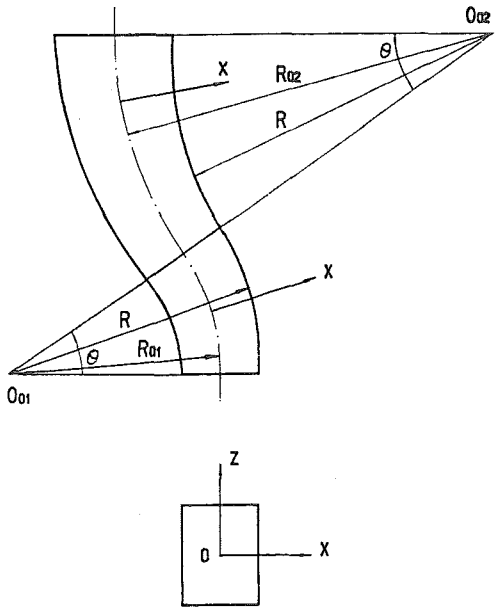

Fig.2 Orthogonal curvilinear coordinates (x,θ,z)

A body–fitted coordinate system (ξ,ζ,η) is set up in the present study. The coordinate directions of ξ and η are shown in Fig.3. ζ axe directs the downstream of the duct flow.

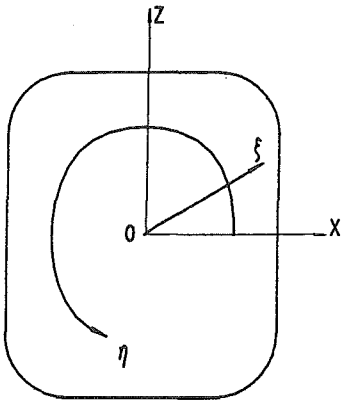

Fig.3 ξ,η coordinates arranged in cross–section

For the flow through an S–duct with variational section as Fig.1, the general governing equation, i.e. Navier–Stokes equation can be expressed in cylindrical coordinats (x,θ,z) as

$$\frac{\partial R\rho u\Phi}{R\partial x}+\frac{\partial \rho v\Phi}{\partial z}+\frac{\partial \rho w\Phi}{R\partial\theta}$$
$$=\frac{\partial}{R\partial x}(\Gamma\frac{\partial R\Phi}{\partial x})+\frac{\partial}{\partial z}(\Gamma\frac{\partial\Phi}{\partial z})+\frac{\partial}{R\partial\theta}(\Gamma\frac{\partial\Phi}{R\partial\theta})+S \quad (1)$$

which is suitable to two bends and the straight part of the S-duct in Fig.1. $R=R_{01}+x$ and $R=R_{02}-x$ for first and second bend respectively, and $R=1$ for the straight part.

In equation (1), ρ is the fluid density. u,v,w are velocity components in x,z,θ directions respectively. Φ is a general variable that may be u,v,w, the kinetic energy of turbulence k and its dissipation rate ε. Γ is exchange coefficient that means dynamic viscosity when Φ represents u,v,w. And S is source terms which are different for different variable Φ.

Eg.(1) can be transformed to (ξ,ζ,η) coordinates with tensor analysis. The transformed N-S equation remains conservative with the help of the conservative transforming relations between (x,θ,z) and (ξ,ζ,η) coordinate systems. It is not only convenient to the numerical solution, but also gives the clear physical meaning. The relations are given as follows.

Let A be equal to a scalar function, and conservative gradient is expressed by[9]

$$\underline{\nabla}A=\frac{1}{J}\sum_{i=1}^{3}(J\,\underline{a}^{i}A)_{\xi^i} \quad (2)$$

where

$$\underline{a}^{i}=\frac{1}{J}e_{ijk}\sum_{m=1}^{3}\sum_{n=1}^{3}\frac{\partial x^m}{\partial\xi^j}\frac{\partial x^n}{\partial\xi^k}\underline{g}_m\times\underline{g}_n \quad (3)$$
$$(i=1,2,3)\quad (i,j,k)\ \text{cyclic}$$

Here, $(\underline{\ \cdot\ })$ is vector. $x^i(i=1,2,3)$ indicates the variables x,θ, z of original coordinates. $\xi^i(i=1,2,3)$ represents the variable ξ,ζ,η of the body-fitted coordinates. $\underline{a}^i(i=1,2,3)$ is the contravariant base vectors of (ξ,ζ,η) coordinates, and $\underline{g}_i(i=1,2,3)$ is the covariant base vectors of (x,θ,z) coordinates. $J=\partial(x,\theta,z)/\partial(\xi,\zeta,\eta)$ is the Jacobian of the transformation. The quantity e_{ijk} shows the permutation symbols, by the rules of tensor analysis.

In cylindrical coordinates (x,θ,z), the relations between $g_i(i=1,2,3)$ and unit vectors $\underline{i}_R,\underline{i}_\theta,\underline{i}_z$ are:

$$\left.\begin{aligned}\underline{g}_1&=\underline{i}_R\\ \underline{g}_2&=R\,\underline{i}_\theta\\ \underline{g}_3&=\underline{i}_z\end{aligned}\right\} \quad (4)$$

and

$$\left.\begin{aligned}&\underline{g}_i\times\underline{g}_i=0 \qquad (i=1,2,3)\\ &\underline{g}_1\times\underline{g}_2=R\,\underline{g}_3\\ &\underline{g}_2\times\underline{g}_3=R\,\underline{g}_1\\ &\underline{g}_3\times\underline{g}_1=\frac{1}{R}\underline{g}_2\end{aligned}\right\} \quad (5)$$

moreover

$$\left.\begin{aligned}(\underline{g}_1)_{\xi^i}&=\frac{\theta_{\xi^i}}{R}\underline{g}_2\\ (\underline{g}_2)_{\xi^i}&=\frac{x_{\xi^i}}{R}\underline{g}_2-R\theta_{\xi^i}\underline{g}_1\\ (\underline{g}_3)_{\xi^i}&=0\end{aligned}\right\} \quad (6)$$

The conservative gradient in (ξ,ζ,η) coordinates derived using Eqs. (3)~(6) in Eq.(2) by expansion is compared with that in (x,θ,z) coordinates, so that the conservative derivative transformation relations between (x,θ,z) and (ξ,ζ,η) coordinate systems can be obtained as follows[10]

$$\left.\begin{aligned}\frac{\partial A}{\partial x}&=\frac{1}{J}\{\frac{1}{2}\sum_{i=1}^{3}\sum_{j=1}^{3}\sum_{k=1}^{3}e_{ijk}[(R\theta_{\xi^j}z_{\xi^k}-R\theta_{\xi^k}z_{\xi^j})A]_{\xi^i}\\ &\quad\mp\frac{A}{R}\}\\ \frac{\partial A}{R\partial\theta}&=\frac{1}{2J}\sum_{i=1}^{3}\sum_{j=1}^{3}\sum_{k=1}^{3}e_{ijk}[(z_{\xi^j}x_{\xi^k}-z_{\xi^k}x_{\xi^j})A]_{\xi^i}\\ \frac{\partial A}{\partial z}&=\frac{1}{2J}\sum_{i=1}^{3}\sum_{j=1}^{3}\sum_{k=1}^{3}e_{ijk}[(x_{\xi^j}R\theta_{\xi^k}-x_{\xi^k}R\theta_{\xi^j})A]_{\xi^i}\end{aligned}\right\} \quad (7)$$

The contravariant components $u^i(i=1,2,3)$ in ξ^idirection of velocity vector $\underline{u}$ for (ξ,ζ,η) coordinates are given by

$$\left.\begin{aligned}u^1&=\frac{1}{J}[(R\theta_\zeta z_\eta-R\theta_\eta z_\zeta)u+(x_\eta z_\zeta-x_\zeta z_\eta)w\\ &\quad+(x_\zeta R\theta_\eta-x_\eta R\theta_\zeta)v]\\ u^2&=\frac{1}{J}[(R\theta_\eta z_\xi-R\theta_\xi z_\eta)u+(x_\xi z_\eta-x_\eta z_\xi)w\\ &\quad+(x_\eta R\theta_\xi-x_\xi R\theta_\eta)v]\\ u^3&=\frac{1}{J}[(R\theta_\xi z_\zeta-R\theta_\zeta z_\xi)u+(x_\zeta z_\xi-x_\xi z_\zeta)w\\ &\quad+(x_\xi R\theta_\zeta-x_\zeta R\theta_\xi)v]\end{aligned}\right\} \quad (8)$$

Eqs. (7) and (8) are applicable to two bends of the S-duct. For the symbol $\mp$, the upper one is suitable for first bend and the lower for second bend.

Ⅲ. Mathematical Model

The Eq.(1) can be transformed conveniently from (x,θ,z) coordinates to (ξ,ζ,η) coordinates by use of Eqs. (7) and (8). It is found that Eqs. (7) and (8) may be simplified in many real situations.

For example, when the centre lines of the two bends of the S-duct are exact or approximate circle arc. The terms θ_ξ and θ_η can be neglected, i.e.

$$\left.\begin{aligned}\theta_\xi&=0\\ \theta_\eta&=0\end{aligned}\right\} \tag{9}$$

If the S-duct has big slender proportion or low-diffusion, there exist the following approximations.

$$\left.\begin{aligned}R\triangle\theta&\approx\triangle\zeta\\ R\theta_\xi&\approx 1\end{aligned}\right\} \tag{10}$$

For the three-dimensional turbulent flow without recirculation in the predominant direction through an S-duct as Fig.1, the diffusion fluxes can be neglected in that direction. However, because of the significant curvature of the duct, the pressure transmission of the flow in upstream direction should be considered. In the present study the partially-parabolized Navier-Stokes equations are employed to describe the flow situation. After transformed from (x,θ,z) coordinates to (ξ,ζ,η) coordinates, Eq.(1) is properly simplified. As a result, the general expression of the governing equations of the flow in the S-duct with arbitrary cross-section is

$$\begin{aligned}&(\rho U\Phi)_\xi+(\rho V\Phi)_\eta+(\rho W\Phi)_\zeta\\ &\quad=\{\frac{\Gamma}{J}[(z_\eta)^2+D^2+(x_\eta)^2]\Phi_\xi\}_\xi\\ &\quad+\{\frac{\Gamma}{J}[(z_\xi)^2+E^2+(x_\xi)^2]\Phi_\eta\}_\eta+JS\end{aligned} \tag{11}$$

Where Φ,ρ,Γ,S have explained in Eq.(1), but the source term S is different from that in Eq.(1) because of the transformations. The other variables in Eq.(11) are:

$$\left.\begin{aligned}U&=Ju^1=z_\eta u-x_\eta v+Dw\\ V&=Ju^2=-z_\xi u+x_\xi v+Ew\\ W&=Ju^3=Jw\\ J&=x_\xi z_\eta-x_\eta z_\xi\\ D&=x_\eta z_\zeta-x_\zeta z_\eta\\ E&=x_\zeta z_\xi-x_\xi z_\zeta\end{aligned}\right\} \tag{12}$$

It is evident that Eq.(11) is analogous to Eq.(1) and also conservative.

The turbulent nature of the flow is described by two equation k-ε turbulence model. And the viscosity is calculated by

$$\mu_t=\frac{c_\mu c_D\rho k^2}{\varepsilon}\quad(c_\mu c_D=0.09) \tag{13}$$

Ⅳ. Grid Generation

Based on above coordinate transformation, the 3-D physical domain can be transformed to generate automatically boundary-fitted meshes that may be extended to the arbitrary case of duct flow. In Fig.1 the cross-section of the entry of the duct is rectangular, which becomes a circle gradually from entry to outlet. The centerline of the duct consists mainly of two opposite planar circular arcs. The equivalent divergence angle of the duct is about 4.722° . Therefore, the coordinate transformation of the 3-D physical domain of the duct can be made by generating two-dimensional body-fitted meshes for every cross-section along the duct one by one.

In the coordinates as Fig.3, the body-fitted grids of each cross-section can be got numerically by means of a set of differential equations

$$\left.\begin{aligned}\nabla^2\xi&=P(x,z)\\ \nabla^2\eta&=Q(x,z)\end{aligned}\right\} \tag{14}$$

Thus, the task of three-dimensional meshs for analysis can be translated into a series of two-dimensional meshes generated in x-z cross-section planes in which the mesh generation is automatically controlled. P and Q in Eq.(14) are the functions of ξ and η. By use of reasonable function P and Q, a satisfactory distribution of the mesh can be obtained for arbitrary shaped cross-section. The numerical mesh of some cross-section of the duct is shown in Fig.4 where physical domain in x-z plane is transformed to regular rectangular domain in ξ-η plane. It is seen that the flow bound coincides with the grids on the bound of the domain. There often exist singular points in generating body-fitted grid for the flow in ducts, such as the centre point O of the section in Fig.4.

In order to solve the problem a additive curve is enclosed around O point as inner bound in the study.

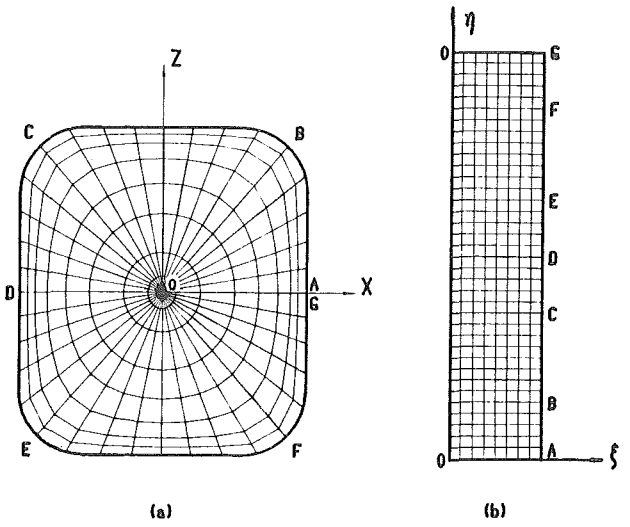

Fig.4 Computational mesh generated in x–z and ξ–η planes

The numerical meshes of several sections along the S–duct are presented in Fig.5.

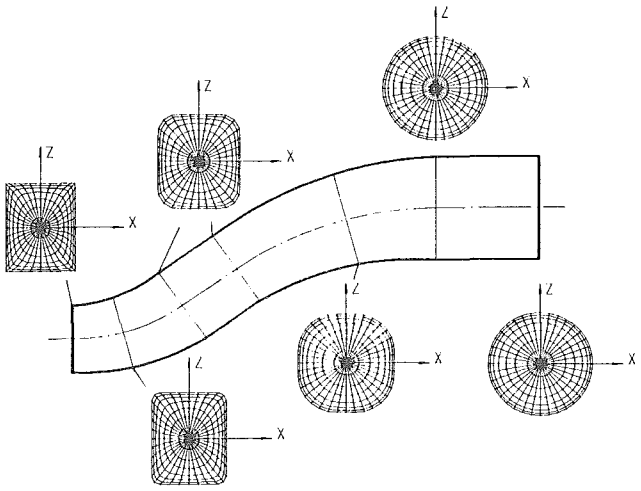

Fig.5 Fitted–body grid generated along the S–duct

V. Numerical Procedure

The three–dimensional turbulent flow field in S–duct has been computed by finite–difference approach in which the governing equation (11) described above is solved numerically.

At first, the difference equations are derived by discreting Eq. (11) on the boundary–fitted mesh in Fig.4. According to the feature of the flow, the partially–parabolized governing equations are used. The flow variables are calculated by marching, through the flow domain along the predominant direction, combined with iteration at each cross–section in sequence from entry to downstream. In the computational approach, the pressure field is stored as three–dimensional array so that the effect of pressure on whole flow field can be transmited by marching repeatedly. And all other variables are stored at any time of marchings as two–dimensional arrays in cross–sectional plane.

It has been proved that U,V and W are velocity components of u respectively in ξ,η and ζ directions[10], while u,v and w are physical velocity components of u respectively in R,z,and θ directions. The staggered grid system is adopted, in which U,V and W are located in the middle of adjacent grids corresponding with the coordinate directions of u,v and w respectively. The other variables are settled on grids. The initial values of u,v,w and p of the flow at the duct entry are gained by experiment[10]. The initial predominant velocity w is 62m / s.

It is known that the values of u,v and w depend on the distribution of the pressure of the flow. With reference to firsthand SIMPLE method[11], some improvement has been done. A new pressure–correction equation for body–fitted coordinates (ξ,ζ,η) has been derived by use of continuity equation. The pressure computed and velocity components u,v and w are corrected with the help of pressure–correction equation in every iteration at each station, in order to get more reasonable distribution of the pressure and velocity field. The correction formulas for the velocity components are written as

$$\left.\begin{aligned} u'_e &= d_e(p'_P - p'_E) + c_e(p'_P - p'_N) \\ u'_w &= d_w(p'_W - p'_P) + c_w(p'_S - p'_P) \\ v'_n &= d_n(p'_P - p'_N) + c_n(p'_P - p'_E) \\ v'_s &= d_s(p'_S - p'_P) + c_s(p'_W - p'_P) \\ w'_p &= d_p p'_P \end{aligned}\right\} \qquad (15)$$

while

$$\left.\begin{aligned} p &= p^* + p' \\ u &= u^* + u' \\ v &= v^* + v' \\ w &= w^* + w' \end{aligned}\right\} \qquad (16)$$

The subscripts stand for the locations of numerical meshes (See Fig.6). The starred variables p^*, u^*, v^* and w^* are the values obtained in last iteration, and u', v', and w' are velocity corrections corresponding to pressure correction p'. The corrected p,u,v and w are taken as the value of the current iteration. The pressure–correction equation can be deduced by substituting Eqs. (15) and (16) into the difference equation of continuity. The coefficients in Eq. (15) are calculated by the difference equations of u,v,w momentum equations.

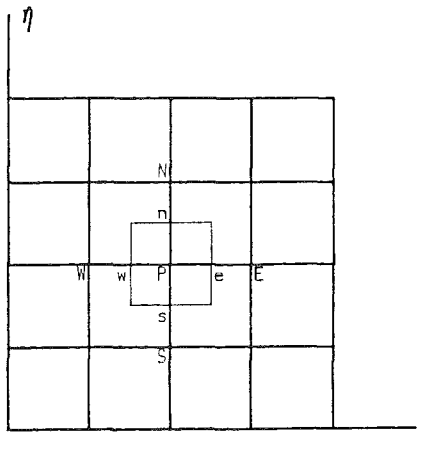

Fig.6 Locations of subscripts of Eq.(15) at ξ–η mesh

By pressure–correction equation, the pressure field is corrected in itself to bring the velocities to conform with the continuity equation. Besides, the pressure distribution and predominant velocity w are also corrected by non–equilibrium of the flow flux between entrance and current station in marching computation. The numerical marching, with iterations in every section of the duct, through the flow domain are repeated many times, using a more correct pressure field each time. The procedure is terminated when the corrections to the pressure field have become so small that the residues of three velocity components and airflow are smaller than a preassigned value.

The center point in every corss–section of the duct is a singular point in the process of grid generation. It is also a problem in the solution of the flow equations. Analytically, the metrics vanish at this point and it makes the flow variables multivalue. In the present study an additive closed bound is made around the inner point. The value of the flow variables at the inner mesh point is equal to the average value of those at grids surrounding the singular point after every iteration. The results prove that the treatment is desirable.

VI. Results and Discussion

Computations for the turbulent flow illustrated in Fig.1 have been made. The flow parameters obtained in the S–shaped duct have fairly good agreement with experimental data[10].

A typical vortex pair of the transverse flow at outlet of the duct appears in Fig.7. The calculating and experimental results show that the corss–sectional flow patterns in Fig.7a and 7b are very similar.

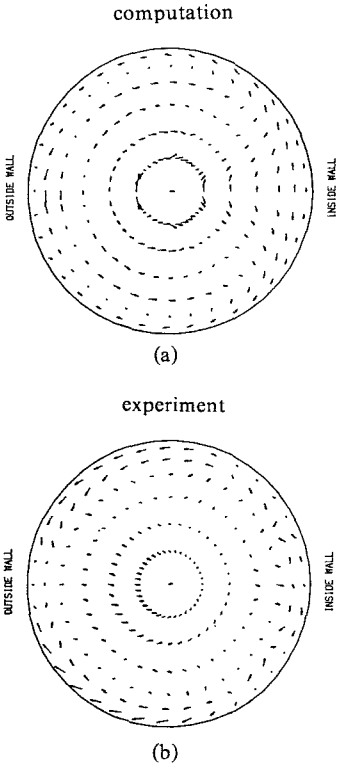

Fig.7 Transverse velocity vectors at outlet section

The distribution of total pressure coefficcent at outlet section is an important property of the flow in aircraft inlets. Fig.8 gives the results of computation and experiment, in which it is seen that the distribution of pressure loss computed looks like the situation of that from experiment. The pressure loss is larger near the wall which is far away from the fuselage and called outside wall in Fig.8a. However, it does not appear in Fig.8b. The reason for this may be that a separation of the flow occurs in second bend near outside wall due to the larger curva-

ture there. But the partially–parabolized solution is only able to analyse the one–way flow.

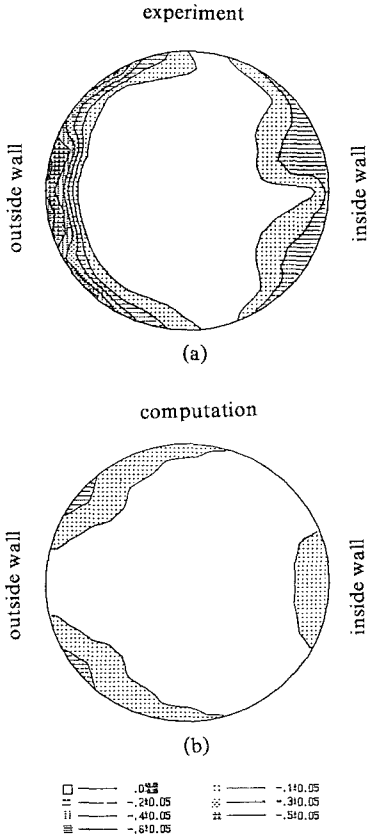

Fig.8 Total pressure coefficients at outlet section

Fig.9 shows the theoretical distributions of static pressure coefficient on the symmetrical line of the duct walls which have the same tendency with those of experiment. The numerical gradient of the static pressure, reflecting the nature of the flow through an S–duct, is correct, though there are some differences in the data.

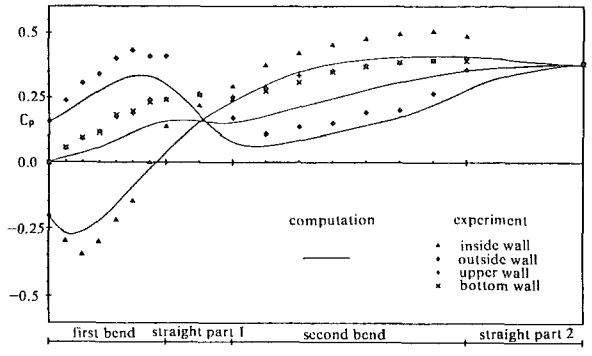

Fig.9 Static pressure coefficients along the S–duct walls

The development of longitudinal velocity w along the S–shaped diffuser is shown in Fig.10 that gives the distribution of w component in symmetrical plane at different sections. Because of the duct diffusion the mean flow velocity decreases along the duct. The analytical result shows the variation of w component in accordance with the curvature of S–duct. Since only the flow field at outlet is measured, a comparison between numerical curve and experimental data at exit setion is given in Fig.10. It is seen that experimental points stand very near the computed velocity profile.

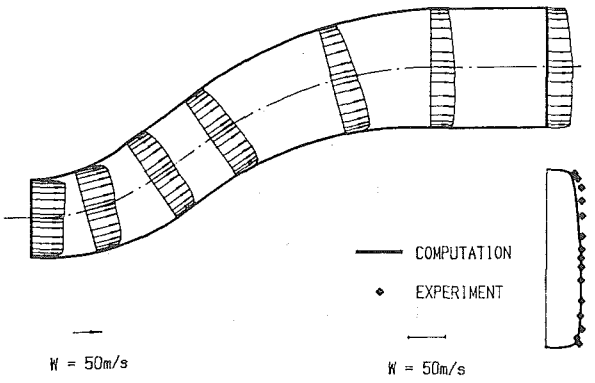

Fig.10 Longitudinal velocity profiles at different sections along the S–duct

Reviewing the foregoing results, it may to be concluded that the mathematic model and numerical procedure considered in the present study are practicable for computing three–dimensional turbulent flow through S–shaped ducts with arbitrary sections. And expectantly, the numerical approach can be spread to 3–D turbulent flow in more complicated ducts.

Refrences

1. Forester, C.K., Body–Fitted 3–D Full–Potential Flow Analysis of Complex Ducts and Inlets. AIAA–81–0002

2. White, J.W., A General Mapping Procedure for Variable Area Duct Acoustics. AIAA–81–0094.

3. Vakili, A., Wu, J.M., Comparision of Experimental and Computational Compressible flow in an S–Duct. AIAA–84–0033.

4. Pratap, V.S., Spalding, D.B., Numerical Computations of the Flow in Curved Ducts. The Aeronautical Quarterly, Aug. 1975.

5. Eiseman, P.R., Levy, R., McDonald, H. & .

Briley, W.R., Development of a Three–Dimensional Turbulent Duct Flow Analysis. NASA CR–3029.

6. Guo, R.W., Lin, Q., Compressible Turbulent Flow in an S–Shaped Diffuser. 5th Int. Conf. on Numerical Methods in Laminar and Turbulent Flow. Montreal, Canada July, 1987.

7. Towne, C.E., Application of Computational Fluid Dynamics to Complex Inlet Ducts. AIAA–85–1213.

8. Povinelli, L.A., Towne, C.E., Viscous Analysis for Flow Through Subsonic and Supersonic Intake. NASA TM 88831, 1986.

9. Thompson, J.F., Warsi, Z.U.A. & Mastin, C.W., Numerical Grid Generation (Foundations and Applications) North–Holland, New York, 1985.

10. Lin, Q., Numerical Analysis and Experimental Investigation for the Characteristics of Flow through a Rectangular–Round S–Shaped Diffuser. Doctoral thesis in Nanjing Aeronautical Institute, 1988.

11. Patanker, S.V., Numerical Heat Transfer and Fluid Flows. McGraw–hill, New York, 1980.